

Metallo drugs

A Rhenium Isonitrile Complex Induces Unfolded Protein Response-Mediated Apoptosis in Cancer Cells

A. Paden King^{+, [a]}, Sierra C. Marker^{+, [a]}, Robert V. Swanda,^[b] Joshua J. Woods,^[a, c] Shu-Bing Qian,^[b] and Justin J. Wilson^{*[a]}

Abstract: Complexes of the element Re have recently been shown to possess promising anticancer activity through mechanisms of action that are distinct from the conventional metal-based drug cisplatin. In this study, we report our investigations on the anticancer activity of the complex $[\text{Re}(\text{CO})_3(\text{dmphen})(p\text{-tol-ICN})]^+$ (TRIP) in which $\text{dmphen} = 2,9\text{-dimethyl-}1,10\text{-phenanthroline}$ and $p\text{-tol-ICN} = para\text{-tolyl isonitrile}$. TRIP was synthesized by literature methods and exhaustively characterized. This compound exhibited potent in vitro anticancer activity in a wide variety of cell lines. Flow cytometry and immunostaining experiments indicated that TRIP induces intrinsic apoptosis. Comprehensive biological mechanistic studies demonstrated that this compound triggers the accumulation of misfolded proteins, which causes endoplasmic reticulum (ER) stress, the unfolded protein response, and apoptotic cell death. Furthermore, TRIP induced hyperphosphorylation of eIF2 α , translation inhibition, mitochondrial fission, and expression of proapoptotic ATF4 and CHOP. These results establish TRIP as a promising anticancer agent based on its potent cytotoxic activity and ability to induce ER stress.

The endoplasmic reticulum (ER) is a major regulator of cancer cell proliferation, metastasis, angiogenesis, and chemotherapy resistance.^[1] Cancer cells often exhibit higher rates of protein synthesis than non-cancer cells, which raises their ER protein load and leads to higher basal levels of ER stress.^[2] To handle this ER stress, cancer cells often employ the unfolded protein response (UPR). The UPR is typically cytoprotective, and its increased activation in cancer cells can cause them to be more virulent and more resistant to chemotherapy.^[3] However, acute

inductions of high levels of ER stress can shift the UPR to activate apoptosis.^[4] The higher basal ER stress levels of cancer cells make them more susceptible than normal cells to apoptosis induction through overactivation of the UPR. Thus, the development of new chemotherapeutic agents that target the ER is a promising strategy for the treatment of cancer.^[5] Recently, several transition-metal complexes bearing polypyridyl ligands have been discovered to induce anticancer activity through ER stress and the UPR, suggesting that the exploration of these nontraditional scaffolds may give rise to promising drug candidates.^[6–11] In this context, our group has been exploring the anticancer activity of polypyridyl rhenium(I) tricarbonyl complexes.^[12–15] Certain members of this class of compounds exhibit potent cytotoxic activity, which can be leveraged for their use as anticancer agents.^[16–23] Here, we describe our investigation of a new rhenium(I) tricarbonyl complex bearing a chelating polypyridyl ligand and an axial isonitrile ligand as a potent anticancer agent. Our efforts to understand the mechanism of action of this tricarbonyl rhenium isonitrile polypyridyl (TRIP) complex (Figure 1) have revealed that it is an effective ER stress-inducing agent with significant antiproliferative activity.

TRIP was synthesized by treating the previously reported complex $[\text{Re}(\text{CO})_3(\text{dmphen})\text{OTf}]$ with excess *para*-tolyl isonitrile in tetrahydrofuran. TRIP was fully characterized using ¹H NMR and IR spectroscopy, high resolution mass spectrometry (HRMS), and X-ray diffraction (Figures S1 and S2, Tables S1 and S2, Supporting Information). The purity of the complex was

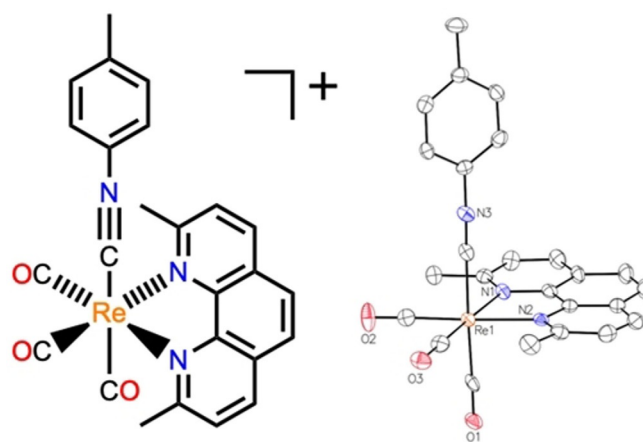


Figure 1. Diagram of TRIP (left) and its X-ray crystal structure (right). Ellipsoids are drawn at 50% probability. Hydrogen atoms and the counterion are omitted for clarity.

[a] A. P. King,⁺ S. C. Marker,⁺ J. J. Woods, Prof. J. J. Wilson
Department of Chemistry and Chemical Biology, Cornell University
Ithaca, NY 14853 (USA)
E-mail: jjw275@cornell.edu

[b] R. V. Swanda, Prof. S.-B. Qian
Division of Nutritional Sciences, Cornell University, Ithaca, NY 14853 (USA)

[c] J. J. Woods
Robert F. Smith School for Chemical and Biomolecular Engineering
Cornell University, Ithaca, NY 14853 (USA)

[⁺] These authors contributed equally to this work.

Supporting information and the ORCID identification number(s) for the author(s) of this article can be found under:
<https://doi.org/10.1002/chem.201902223>.

verified by elemental analysis and HPLC (Figure S3, Table S3, Supporting Information). The water-soluble complex is luminescent upon irradiation with UVA and blue light and exhibits a luminescence quantum yield of 3% and a lifetime of 1.05 μ s in aqueous, air-equilibrated phosphate buffer (Figures S4–S6, Supporting Information). The complex is stable indefinitely as a solid and in aqueous solution for over one week (Figures S7 and S8, Supporting Information). TRIP is also stable in the presence of millimolar concentrations of glutathione (Figure S9, Supporting Information). Based on the favorable physical properties and high stability of TRIP, we evaluated its potential as an anticancer agent *in vitro*.

The cytotoxicity of TRIP was investigated in a panel of cancer and non-cancer cell lines to determine its potential as a therapeutic agent. For comparison, we also evaluated the activities of the established metal-based anticancer drug cisplatin and another potent rhenium anticancer agent that we have previously investigated in our lab, $[\text{Re}(\text{CO})_3(\text{dmphen})(\text{OH}_2)]^+$ (Neo-Re).^[12,15] The concentrations of these complexes required to reduce cell viability to 50% of the control (IC_{50}) are shown in Table 1. In comparison to cisplatin and Neo-Re, TRIP has

Table 1. IC_{50} values of TRIP, Neo-Re, and cisplatin in cancer and non-cancer cell lines.

Compound	IC_{50} [μM]				
	A2780 ^[a]	A2780CP70 ^[b]	HeLa ^[c]	A549 ^[d]	HEK293 ^[e]
TRIP	1.7 \pm 0.7	1.9 \pm 1	1.4 \pm 0.2	1.4 \pm 0.6	1.9 \pm 0.2
Neo-Re	5.7 \pm 0.6	6.0 \pm 0.2	4.4 \pm 1.3	7.7 \pm 2.4	9.0 \pm 0.3
Cisplatin	1.3 \pm 0.1	12 \pm 3	6.6 \pm 0.7	5.6 \pm 0.5	1.7 \pm 0.2

[a] Ovarian cancer. [b] Cisplatin-resistant ovarian cancer. [c] Cervical cancer. [d] Lung cancer. [e] Embryonic kidney fibroblasts.

comparable or greater toxicity in all cancer cell lines tested (Figures S10–S21, Supporting Information). Based on its promising anticancer activity, we submitted TRIP for screening in the National Cancer Institute (NCI)-60 cell line panel (Figure S22, Supporting Information).^[24] The results indicate that TRIP is most potent in melanoma and breast cancer cell lines and least effective in lung and renal cancer cell lines. The activity of TRIP in this cell line panel was compared to drugs in the NCI database through the COMPARE algorithm, which compares the toxicity profiles of drugs to reveal correlations in their activity.^[25] Highest correlations were observed for DNA-binding agents chromomycin A3 and actinomycin D and the translation inhibitors pyllanthoside, bruceantin, and didemnin B (Table S4, Supporting Information). Notably, the spectrum of activity of TRIP was not correlated to any of the platinum-based drugs, and it exhibits only a moderate correlation ($\text{PCC} = 0.403$) to Neo-Re. The high correlations to established transcription and translation inhibitors indicates that TRIP may act similarly.

To determine the type of cell death induced by TRIP, the cytotoxicity of this compound in A2780 cells was evaluated in the presence of inhibitors of various established cell death pathways. Inhibitors of necroptosis, paraptosis, and ferroptosis did not alter TRIP's activity, but the pan-caspase inhibitor Z-

VAD-FMK significantly decreased TRIP's cytotoxicity (Figures S23–S27, Supporting Information). Considering that the activation of caspases is often critical for the execution of apoptosis, this result indicates that TRIP may be inducing this form of cell death. To confirm that TRIP induces caspase-dependent apoptosis, we first performed western blots to detect apoptosis markers caspase 3 and cleaved PARP (Figure S28, Supporting Information). We further verified this cell death pathway by performing the annexin V assay, which selectively stains apoptotic cells (Figures S29 and S30, Supporting Information). To determine whether TRIP induced apoptosis by the intrinsic pathway, the release of cytochrome *c* from the mitochondria was tracked using flow cytometry (Figure S31, Supporting Information). Cytochrome *c* release occurs on the same time scale as apoptosis induction by TRIP, indicating that TRIP induces intrinsic apoptosis.

Given the promising activity of TRIP in a variety of cancer cell lines and its ability to induce intrinsic apoptosis, we explored its intracellular localization and early cellular effects. The localization of TRIP was probed by measuring the colocalization of TRIP luminescence with organelle-specific fluorescent small molecules or fusion proteins. Partial colocalization was observed with the LysoTracker Red dye and GalT-dsRed fusion protein, but the majority of TRIP luminescence was cytosolic (Figure S32, Supporting Information). While performing these colocalization studies, we observed that the mitochondrial morphology was noticeably altered in TRIP-treated cells. The mitochondria were noticeably rounded and punctate after TRIP treatment, in contrast to the tubular, elongated morphology within untreated cells. Time-lapse microscopy experiments revealed that TRIP induces these changes after only 30 min of treatment in HeLa cells (Figures 2 and S33; Movies S1–S6, Supporting Information). Although TRIP-treated mitochondria were visually different, mitochondrial polarization experiments with the ratiometric sensor JC-1 indicated that the mitochondria remained functional (Figures S34 and S35, Supporting Information), demonstrating that the observed changes might be controlled mitochondrial fission rather than fragmentation. These morphology changes were curtailed in the presence of Mdivi-1, which inhibits dynamin-related protein 1 (Drp1), an essential mediator of fission, confirming that this process is due to mitochondrial fission (Figure 2).^[26] Considering that mitochondrial fission is often associated with autophagy,^[27] we examined the expression of LC3, an autophagosome marker,^[28] in A2780 cells upon treatment with TRIP. After 24 h, a large increase in LC3II expression relative to LC3I was observed in cells treated with TRIP (Figure S36, Supporting Information). Based on these results, it is clear that TRIP induces both autophagy and apoptosis. Given that TRIP does not depolarize the mitochondria or cause release of cytochrome *c* on short time scales, we hypothesized that a different organelle, such as the ER, may be the key target of this compound.

Given the potential connections between mitochondrial fission, autophagy, and ER stress, we explored the effects of the ER stress modulator salubrinal on the cytotoxicity of TRIP in A2780 cells.^[29] Salubrinal operates by inhibiting dephosphorylation of the master regulatory protein eukaryotic initiation

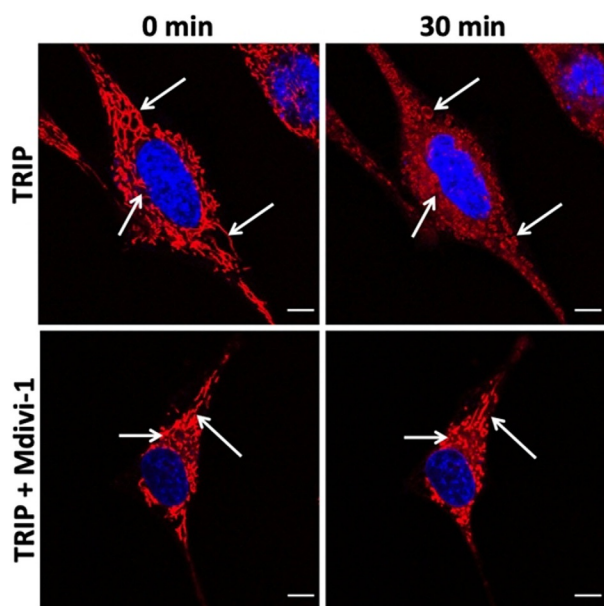


Figure 2. HeLa cells stained with MitoTracker Red (red) and Hoechst dye (blue) treated with TRIP (5 μM) for 0 and 30 min (top panels). HeLa cells stained with MitoTracker Red (red) and Hoechst dye (blue) cotreated with TRIP (5 μM) and Mdivi-1 (50 μM) for 0 and 30 min (bottom panels). Scale bar = 10 μm .

factor 2 α (eIF2 α), which is an integral component of the UPR.^[29–32] The presence of salubrinal increases the activity of TRIP by a factor of 4 (Figure 3A). Based on this synergy, we explored the possibility that TRIP was acting to cause phosphorylation of eIF2 α . Western blot analysis of A2780 cells treated with TRIP confirms the induction of eIF2 α phosphorylation as little as 2 h after exposure (Figures 3B and Figure S37, Supporting Information), indicating that this process is one of the first cellular responses. Next, we explored the downstream effects of eIF2 α phosphorylation. The most immediate and pronounced effect of eIF2 α phosphorylation is the inhibition of translation.^[33] To probe whether the levels of phosphorylation induced by TRIP were sufficient to inhibit protein translation, we measured endogenous global translation levels by using the puromycin incorporation assay.^[34] As early as 2 h post incubation, A2780 cells treated with TRIP incorporated substantially less puromycin compared to the untreated controls, indicating much lower rates of translation (Figure 3C). The role of eIF2 α in these processes was confirmed by testing TRIP in a mutant MEF cell line incapable of eIF2 α phosphorylation. The mutant cells showed no changes in translation levels after TRIP treatment (Figures S38 and S39, Supporting Information).

Hyperphosphorylation of eIF2 α can lead to apoptosis through upregulation of the stress-related transcription factors ATF4 and CHOP.^[35] We measured the upregulation of these

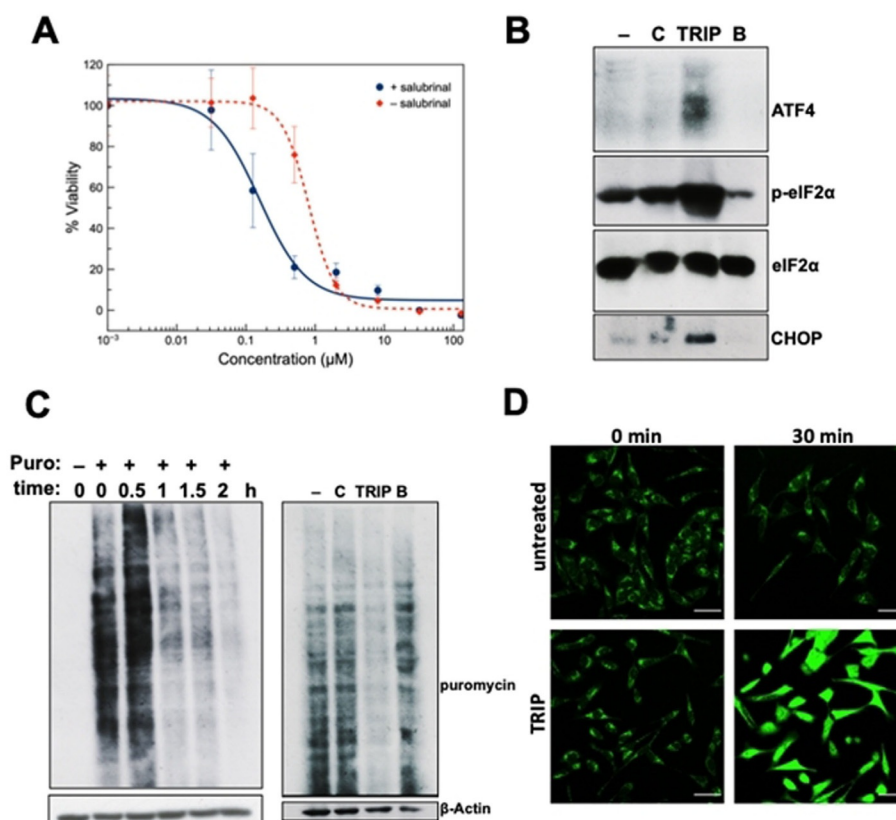


Figure 3. (A) Dose-response curve of A2780 cells treated with TRIP in the presence of 25 μM salubrinal (blue) or absence of salubrinal (red). (B) Western blot of untreated (–), cisplatin (C, 10 μM), TRIP (5 μM), or bortezomib (B, 25 nM) for 24 h in A2780 cells. (C) Western blot of A2780 cells incubated with TRIP (5 μM) over 0, 0.5, 1, 1.5, and 2 h with puromycin (10 min, left blot) and A2780 cells untreated (–), cisplatin (C, 10 μM), TRIP (5 μM), or bortezomib (B, 25 nM) treated for 24 h with puromycin (10 min, right blot). (D) Confocal microscopy images of HeLa cells treated with ThT (5 μM) at 0 and 30 min in the absence (top panels) and the presence (bottom panels) of TRIP (5 μM) at 0 and 30 min. Scale bar = 50 μm .

proteins in response to TRIP treatment and found that both ATF4 and CHOP were upregulated (Figure 3B), linking the observed eIF2 α phosphorylation and apoptosis. Phosphorylation of eIF2 α also results in cell cycle arrest in the G1 phase.^[36] Cells treated with TRIP showed an 18% increase in the population of cells in the G1 phase and a corresponding decrease in the number of cells in the S phase as opposed to untreated cells (Figure S40, Supporting Information). Thus, the ability of TRIP to stall cells in the G1 phase is fully consistent with its induction of eIF2 α phosphorylation. These results indicate that TRIP induces ER stress, triggering eIF2 α phosphorylation and the resulting downstream effects, culminating in cellular apoptosis.

Phosphorylation of eIF2 α often occurs due to the accumulation of misfolded proteins. To determine whether the observed phosphorylation was due to protein misfolding, the extent of misfolded protein accumulation induced by TRIP was evaluated by using the dye thioflavin T (ThT), which fluoresces in the presence of protein aggregates.^[37] The fluorescence intensity of ThT increased significantly in HeLa cells treated with TRIP or the positive control bortezomib in comparison to untreated cells and cells treated with cisplatin within 30 min (Figure 3D; Figures S41 and S42, Movies S7–S10, Supporting Information). Given the observation of fast protein aggregation upon treatment with TRIP, the induction of protein misfolding is most likely the cause of the ER stress and activation of the UPR.

A summary of our current understanding of TRIP's mechanism of ER stress induction and the subsequent cellular response is shown in Figure 4. TRIP induces ER stress in less than 30 min after exposure, due to the accumulation of misfolded proteins. Misfolded protein accumulation leads to the phosphorylation of eIF2 α , which initiates autophagy, shuts down global protein translation, and upregulates ATF4. Prolonged eIF2 α phosphorylation and upregulation of ATF4 leads to expression of the proapoptotic protein CHOP, which induces mi-

tochondrial membrane depolarization and release of cytochrome *c*. This release then results in caspase activation and initiation of apoptosis. Although we have investigated potential causes of eIF2 α phosphorylation, including proteasome inhibition, HSP90 inhibition, and reactive oxygen species generation, we found no evidence that TRIP triggers protein misfolding through these pathways (Figures S43–S47, Supporting Information). Recently, a range of diverse metal complexes have been shown to induce ER stress.^[7–11,38–47] The major mechanism of action proposed for these agents is through the production of reactive oxygen species (ROS). Only a few studies have discovered metal complexes that induce ER stress in the absence of ROS generation.^[9,38,39,48] The ability of TRIP to induce ER stress independent of ROS generation indicates that it operates via a different mechanism than many other metallo drugs targeting the ER.

Collectively, these results establish TRIP as a promising anti-cancer agent that kills cells by causing the accumulation of misfolded proteins. The favorable physical and photophysical properties of TRIP, as well as its high potency, make it a candidate for future studies and a platform for the design of more potent analogues. Our current efforts are directed toward synthesizing a variety of related complexes to develop a structure–activity relationship and performing proteomics studies to identify TRIP's molecular mechanism of action.

Experimental Section

Complex synthesis, characterization, and biological evaluation

The Supporting Information for this article contains all experimental procedures and data.

Crystallographic data

CCDC 1902045 contains the supplementary crystallographic data for this paper. These data are provided free of charge by The Cambridge Crystallographic Data Centre.

Acknowledgements

This research was supported by the College of Arts and Sciences at Cornell University, the Cornell Technology Licensing Office Cornell Technology Acceleration and Maturation (CTAM) fund, and by the Office of the Assistant Secretary of Defense for Health Affairs through the Ovarian Cancer Research Program under award no. W81XWH-17-1-0097. This work made use of the NMR facility at Cornell University, which is supported, in part, by the NSF under award number CHE-1531632. A.P.K. and R.S. thank the National Institute of Health, National Institute of General Medical Sciences, for a Chemical Biology Interface (CBI) Training Grant (grant number T32GM008500). Work in the lab of S.-B.Q. is supported by NIH grants R01GM1222814 and R21CA227917 and by the Howard Hughes Medical Institute (award number 55108556). J.J.W. is supported by the NSFGRFP (DGE-1650441). We thank the BRC imaging fa-

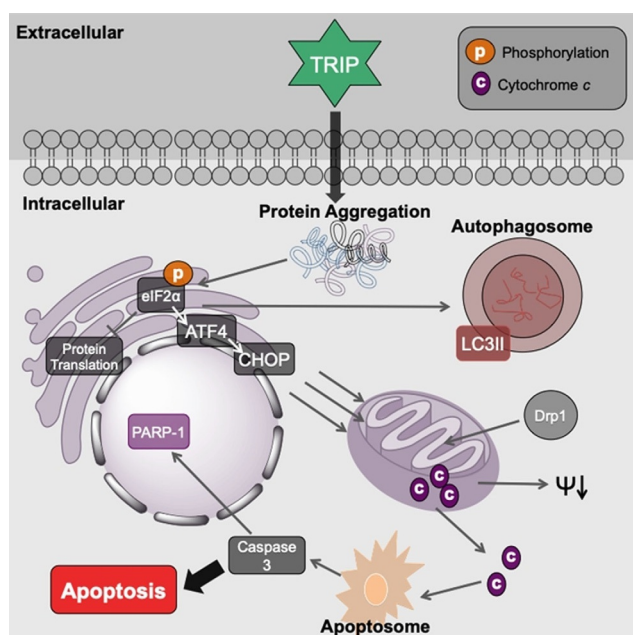


Figure 4. Proposed mechanism of ER stress and apoptosis induction by TRIP.

cility at Cornell University for help with flow cytometry experiments. We also thank Prof. Warren Zipfel and Prof. Jeremy Baskin for assistance with the fluorescence decay lifetime measurements and allowing us to use their confocal fluorescence microscope for acquiring all the live cell images, respectively. Ms. Sam Davalos is thanked for assistance in preparing the Table of Contents figure.

Conflict of interest

The authors declare no conflict of interest.

Keywords: bioinorganic chemistry · cancer · endoplasmic reticulum stress · metallodrugs · translation inhibition

- [1] H. Urrea, E. Dufey, T. Avril, E. Chevet, C. Hetz, *Trends Cancer* **2016**, *2*, 252–262.
- [2] Y.-P. Vandewynckel, D. Laukens, A. Geerts, E. Bogaerts, A. Paridaens, X. Verhelst, S. Janssens, F. Heindryckx, H. Van Vlierberghe, *Anticancer Res.* **2013**, *33*, 4683–4694.
- [3] M. J. Mann, L. M. Hendershot, *Cancer Biol. Ther.* **2006**, *5*, 736–740.
- [4] R. Sano, J. C. Reed, *Biochim. Biophys. Acta Mol. Cell Res.* **2013**, *1833*, 3460–3470.
- [5] R. Ojha, R. K. Amaravadi, *Pharmacol. Res.* **2017**, *120*, 258–266.
- [6] J. Pracharova, G. Viguera, V. Novohradsky, N. Cutillas, C. Janiak, H. Kostrhunova, J. Kasparkova, J. Ruiz, V. Brabec, *Chem. Eur. J.* **2018**, *24*, 4607–4619.
- [7] R. Cao, J. Jia, X. Ma, M. Zhou, H. Fei, *J. Med. Chem.* **2013**, *56*, 3636–3644.
- [8] T. Zou, C.-N. Lok, Y. M. E. Fung, C.-M. Che, *Chem. Commun.* **2013**, *49*, 5423–5425.
- [9] X. Meng, M. L. Leyva, M. Jenny, I. Gross, S. Benosman, B. Fricker, S. Harlepp, P. Hébraud, A. Boos, P. Wlosik, P. Bischoff, C. Sirlin, M. Pfeffer, J.-P. Loeffler, C. Gaiddon, *Cancer Res.* **2009**, *69*, 5458–5466.
- [10] J. S. Nam, M.-G. Kang, J. Kang, S.-Y. Park, S. J. C. Lee, H.-T. Kim, J. K. Seo, O.-H. Kwon, M. H. Lim, H.-W. Rhee, T.-H. Kwon, *J. Am. Chem. Soc.* **2016**, *138*, 10968–10977.
- [11] K. Suntharalingam, T. C. Johnstone, P. M. Bruno, W. Lin, M. T. Hemann, S. J. Lippard, *J. Am. Chem. Soc.* **2013**, *135*, 14060–14063.
- [12] K. M. Knopf, B. L. Murphy, S. N. MacMillan, J. M. Baskin, M. P. Barr, E. Boros, J. J. Wilson, *J. Am. Chem. Soc.* **2017**, *139*, 14302–14314.
- [13] S. C. Marker, S. N. MacMillan, W. R. Zipfel, Z. Li, P. C. Ford, J. J. Wilson, *Inorg. Chem.* **2018**, *57*, 1311–1331.
- [14] C. C. Konkankit, B. A. Vaughn, S. N. MacMillan, E. Boros, J. J. Wilson, *Inorg. Chem.* **2019**, *58*, 3895–3909.
- [15] C. C. Konkankit, A. P. King, K. M. Knopf, T. L. Southard, J. J. Wilson, *ACS Med. Chem. Lett.* **2019**, *10*, 822–827.
- [16] C. C. Konkankit, S. C. Marker, K. M. Knopf, J. J. Wilson, *Dalton Trans.* **2018**, *47*, 9934–9974.
- [17] P. V. Simpson, I. Casari, S. Paternoster, B. W. Skelton, M. Falasca, M. Massi, *Chem. Eur. J.* **2017**, *23*, 6518–6521.
- [18] N. Agorastos, L. Borsig, A. Renard, P. Antoni, G. Viola, B. Spingler, P. Kurz, R. Alberto, *Chem. Eur. J.* **2007**, *13*, 3842–3852.
- [19] A. Kurzwernhart, W. Kandjoller, C. Bartel, S. Bächler, R. Trondl, G. Mühlgassner, M. A. Jakupec, V. B. Arion, D. Marko, B. K. Keppler, C. G. Hartinger, *Chem. Commun.* **2012**, *48*, 4839–4841.
- [20] S. Imstepf, V. Pierroz, R. Rubbiani, M. Felber, T. Fox, G. Gasser, R. Alberto, *Angew. Chem. Int. Ed.* **2016**, *55*, 2792–2795; *Angew. Chem.* **2016**, *128*, 2842–2845.
- [21] E. Kottelat, V. Chabert, A. Crochet, K. M. Fromm, F. Zobi, *Eur. J. Inorg. Chem.* **2015**, 5628–5638.
- [22] A. Leonidova, V. Pierroz, R. Rubbiani, J. Heier, S. Ferrari, G. Gasser, *Dalton Trans.* **2014**, *43*, 4287–4294.
- [23] A. Leonidova, G. Gasser, *ACS Chem. Biol.* **2014**, *9*, 2180–2193.
- [24] R. H. Shoemaker, *Nat. Rev. Cancer* **2006**, *6*, 813–823.
- [25] D. W. Zaharevitz, S. L. Holbeck, C. Bowerman, P. A. Svetlik, *J. Mol. Graphics Modelling* **2002**, *20*, 297–303.
- [26] A. Cassidy-Stone, J. E. Chipuk, E. Ingberman, C. Song, C. Yoo, T. Kuwana, M. J. Kurth, J. T. Shaw, J. E. Hinshaw, D. R. Green, J. Nunnari, *Dev. Cell* **2008**, *14*, 193–204.
- [27] M. Niu, X. Dai, W. Zou, X. Yu, W. Teng, Q. Chen, X. Sun, W. Yu, H. Ma, P. Liu, *Transl. Neurosci.* **2017**, *8*, 37–48.
- [28] I. Tanida, T. Ueno, E. Kominami, *LC3 and Autophagy, in Methods in Molecular Biology*, Humana, Albuquerque, **2008**, Vol. 445, pp. 77–88.
- [29] M. Boyce, K. F. Bryant, C. Jousse, K. Long, H. P. Harding, D. Scheuner, R. J. Kaufman, D. Ma, D. M. Coen, D. Ron, J. Yuan, *Science* **2005**, *307*, 935–939.
- [30] K. Pakos-Zebrucka, I. Koryga, K. Mnich, M. Ljujic, A. Samali, A. M. Gorman, *EMBO Rep.* **2016**, *17*, 1374–1395.
- [31] B. F. Teske, S. A. Wek, P. Bunpo, J. K. Cundiff, J. N. McClintick, T. G. Anthony, R. C. Wek, *Mol. Biol. Cell* **2011**, *22*, 4390–4405.
- [32] J. B. DuRose, D. Scheuner, R. J. Kaufman, L. I. Rothblum, M. Niwa, *Mol. Cell. Biol.* **2009**, *29*, 4295–4307.
- [33] S. R. Kimball, *Int. J. Biochem. Cell Biol.* **1999**, *31*, 25–29.
- [34] E. K. Schmidt, G. Clavarino, M. Ceppi, P. Pierre, *Nat. Methods* **2009**, *6*, 275–277.
- [35] H. Matsumoto, S. Miyazaki, S. Matsuyama, M. Takeda, M. Kawano, H. Nakagawa, K. Nishimura, S. Matsuo, *Biol. Open* **2013**, *2*, 1084–1090.
- [36] J. W. Brewer, J. A. Diehl, *Proc. Natl. Acad. Sci. USA* **2000**, *97*, 12625–12630.
- [37] D. R. Beriault, G. H. Werstuck, *Biochim. Biophys. Acta Mol. Cell Res.* **2013**, *1833*, 2293–2301.
- [38] M. J. Chow, C. Licon, G. Pastorin, G. Mellitzer, W. H. Ang, C. Gaiddon, *Chem. Sci.* **2016**, *7*, 4117–4124.
- [39] M. J. Chow, M. V. Babak, K. W. Tan, M. C. Cheong, G. Pastorin, C. Gaiddon, W. H. Ang, *Mol. Pharm.* **2018**, *15*, 3020–3031.
- [40] F.-Y. Wang, X.-M. Tang, X. Wang, K.-B. Huang, H.-W. Feng, Z.-F. Chen, Y.-N. Liu, H. Liang, *Eur. J. Med. Chem.* **2018**, *155*, 639–650.
- [41] X. Wang, Q. Guo, L. Tao, L. Zhao, Y. Chen, T. An, Z. Chen, R. Fu, *Mol. Carcinog.* **2017**, *56*, 218–231.
- [42] S. Mandal, D. K. Poria, R. Ghosh, P. S. Ray, P. Gupta, *Dalton Trans.* **2014**, *43*, 17463–17474.
- [43] T.-L. Lam, K.-C. Tong, C. Yang, W.-L. Kwong, X. Guan, M.-D. Li, V. K.-Y. Lo, S. L.-F. Chan, D. L. Phillips, C.-N. Lok, C.-M. Che, *Chem. Sci.* **2019**, *10*, 293–309.
- [44] J. Zhao, S. Li, X. Wang, G. Xu, S. Gou, *Inorg. Chem.* **2019**, *58*, 2208–2217.
- [45] W.-L. Kwong, R. W.-Y. Sun, C.-N. Lok, F.-M. Siu, S.-Y. Wong, K.-H. Low, C.-M. Che, *Chem. Sci.* **2013**, *4*, 747–754.
- [46] K.-B. Huang, F.-Y. Wang, X.-M. Tang, H.-W. Feng, Z.-F. Chen, Y.-C. Liu, Y.-N. Liu, H. Liang, *J. Med. Chem.* **2018**, *61*, 3478–3490.
- [47] Y. Wang, J. Hu, Y. Cai, S. Xu, B. Weng, K. Peng, X. Wei, T. Wei, H. Zhou, X. Li, G. Liang, *J. Med. Chem.* **2013**, *56*, 9601–9611.
- [48] S. Tardito, C. Isella, E. Medico, L. Marchiò, E. Bevilacqua, M. Hatzoglou, O. Bussolati, R. Franchi-Gazzola, *J. Biol. Chem.* **2009**, *284*, 24306–24319.

Manuscript received: May 14, 2019

Accepted manuscript online: May 15, 2019

Version of record online: June 26, 2019